

# Quantifying flake scar patterning on cores using 3D recording techniques

Chris Clarkson<sup>a,\*</sup>, Lucio Vinicius<sup>b</sup>, Marta Mirazón Lahr<sup>b</sup>

<sup>a</sup> School of Social Science, The University of Queensland, St Lucia, Qld 4067, Australia

<sup>b</sup> Leverhulme Centre for Human Evolutionary Studies, Department of Biological Anthropology, University of Cambridge, Downing Street, Cambridge CB2 3DZ, UK

Received 29 October 2004; received in revised form 27 June 2005; accepted 1 July 2005

## Abstract

A key feature of stone artefact morphology is the arrangement and patterning of negative flake scars left on flakes and cores. Scar patterning is often treated as a rough guide to identifying methods of core preparation and reduction and usually forms a key component of lithic typologies and other systems of analysis. However, scar patterns are often complex and difficult to capture using traditional measurement or classificatory techniques, particularly where flakes are thick and irregular, or where cores are flaked on many sides from a number of platforms. Three-dimensional analysis of flake scars is now more feasible using digital 3D surface scanning technologies, or using three-dimensional measurement tools such as the Microscribe-3DX which is now widely used in biological geometric morphometric studies more generally [D.C. Adams, F.J. Rohlf, D.E. Slice, *Ital. J. Zool.* 71 (2004) 5–16; F.J. Rohlf, L.F. Marcus, *Trends Ecol. Evol.* 8 (1993) 129–132. [1,34]]. This paper develops a mathematical formula for describing scar patterning using vectors calculated from the start and end points of flake scars recorded in three dimensions. Crown Copyright © 2005 Published by Elsevier Ltd. All rights reserved.

*Keywords:* Lithic technology; Microscribe; Core form; Scar patterning; Three-dimensional recording; Vector analysis

## 1. Introduction

Lithic studies are undergoing a period of rapid development. In particular, greater emphasis is now being placed on developing quantitative approaches to analysis, including measures of reduction intensity [8,15,20,21,26], quantitative means of distinguishing between reduction techniques [2,3,27–30,32,37,42,43], new ways of quantifying artefact shape [14,25,36] and more sophisticated multivariate modelling of the fracture path [9–12,15–17,24,31–33,38–41]. This paper continues this trend by offering a new technique for quantifying variation in scar patterning on flakes and cores. Quantitative analysis offers an alternative to the

ambiguity and regionality of conventional typology, and provides results that lend themselves to inter-assemblage comparison while also being amenable to many different kinds of statistical analysis.

Scar patterning is an aspect of artefact morphology that has not received much attention in quantitative terms. Typically, scar patterns are classified according to one of a number of categories ranging from centripetal to parallel to random/undeveloped, and in practise are usually assigned by reference to illustrations of ideal specimens [e.g. 4,6,13]. While this approach is likely to be sufficient for some purposes, it is not as versatile or satisfying as a quantitative measure capable of depicting variation and continuums in scar patterning in any assemblage, region or time period, or of measuring similarity or difference between individual artefacts or whole assemblages.

\* Corresponding author.

E-mail address: [c.clarkson@uq.edu.au](mailto:c.clarkson@uq.edu.au) (C. Clarkson).

In this paper, we develop a methodology for recording scar patterns in three dimensions using a 3D digitiser, the Microscribe-3DX made by Immersion Corporation. We also derive a mathematical formula that converts start and end points for each flake scar recorded in three dimensions into vectors, and thence into an angle that expresses the degree to which scar orientations range between random, centripetal or parallel for a single artefact. A population of 55 experimental and archaeological cores are analysed for a case study that explores the potential of this method to accurately differentiate between flake scar patterns for common core forms. The description of cores is not only a fundamental component of any thorough technological or typological analysis, but the emergence and spread of different core technologies has also been central to recent debates about the appearance and dispersal of various hominin taxa [18,19,23]. Whether core technologies contain information about such events or not, the development of techniques that are better able to capture variation in core form and reduction technology will provide data that are more amenable to answering questions of many kinds, including those concerning technological continuity and change. Since quantitative data of this kind are capable of revealing patterning at finer scales than are traditional typological analyses, the development of such approaches to core analysis is highly desirable at this time.

## 2. Scar patterns and core shape

Scar patterning is perhaps the most direct means we have of determining the techniques and ordering of procedures used in the manufacture of stone artefacts when the actual knapping behaviour cannot be directly observed. Scar patterning is the combined effect of many blows positioned over the surfaces of artefacts and can usually be read in ways that tell us something about the size of flakes removed, the degree of force and type of indenter used, the angle of intersection of faces and the amount of force required, the likely method of core stabilisation, points at which blows went awry, procedures used to maintain or correct core geometry, and many other aspects besides – in sum, the various means by which humans exploited the geometry of artefacts to provide useable tools. Furthermore, these manufacturing procedures are culturally transmitted – both vertically and horizontally – and can convey information about ancestor–descendant relations and inter-group contacts. This creates the potential to document the phylogeny of manufacturing traditions, the nature and rate of change in different cultural, demographic and environmental contexts, the transmission of lithic production norms over wide areas (whether expressing the movement of peoples or ideas), as well as answering

a wide range of questions about past human behaviour. Scar patterning is obviously just one facet of this story of changing technology and adaptation, but because it is often fundamental to interpreting the lithic record, it is well worth developing methods for quantifying variation in this important attribute.

Scar patterns are often closely tied to the geometry of cores, and are therefore also often informative about broad patterns of core reduction. While cores can at times appear totally amorphous – as for example when there is an absence of symmetry in any plane, or of any readily identifiable shape – there are nevertheless strong and recurrent associations between certain core shapes and scar patterns. This is likely to be the result of both the mechanical constraints on stone fracture, which means that cores will tend to coalesce on similar forms (generally dictated by edge angles, force variables, platform variables and inertia), as well as the fact that people typically attempt to create useable flakes while minimising damage to the nucleus that might jeopardise future flake removals. It is likely that this combination of factors often caused convergence in reduction technologies and thus created homoplastic patterns in the archaeological record that reflect functional constraints and considerations. It is also likely that some core classifications, such as those that attempt to pick up on common associations between repeated forms of scar patterning and identifiable core shapes, reflect such functional convergences.

Some of these apparent regularities and associations are illustrated in Fig. 1. This figure combines scar patterns such as parallel, tapering, random, centripetal or bi-centripetal, with a range of common core shapes. The resulting combinations will be familiar to most lithic analysts.

One major advantage of developing a quantitative description of scar patterning, therefore, is to document such associations so that they can be effectively explored in multivariate analyses, leading to more robust, detailed and readily comparable descriptions of core morphology than are currently available.

Prior attempts to quantify flake scar patterning in some way have tended to work in two dimensions only, and therefore fail to capture the complexity of scar patterning found on cores [5,20,22]. Some consideration of core scar patterning is also usually embedded within conventional typological distinctions, with classes often representing a combination of core shape and scar pattern. Scar patterning is obviously a key discriminating trait in the formation of such classes as discoidal cores, polyhedrons, handaxes, pyramidal or bidirectional blade cores, bipolar cores etc. Clark's [6] typological system is a good example of attempts to capture scar patterning using many different idealized core forms. Some core taxonomies even specifically target scar patterning as the central classifying criterion, such as

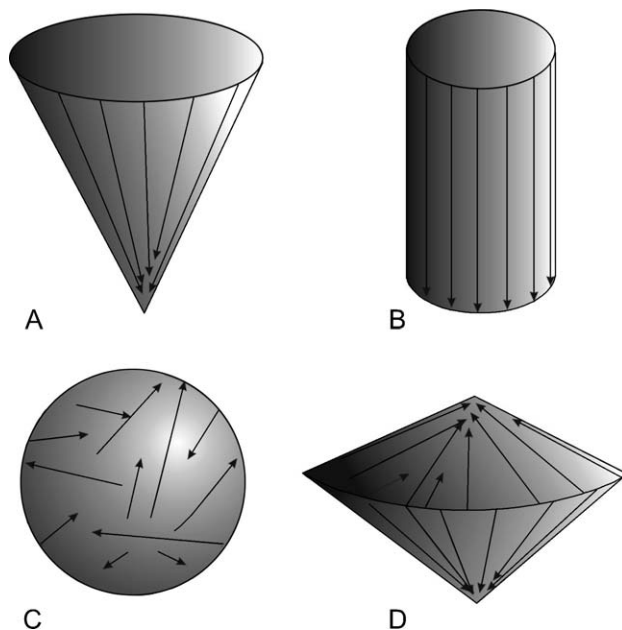


Fig. 1. Various scar pattern arrangements and some likely associations with particular core shapes. A and B are commonly associated with blade technologies and single platform core reduction, C with unsystematic core rotation and the formation of 'polyhedrons', and D with bifaces, discoidal and Levallois-like cores.

Conard et al.'s [9] system which uses categories like inclined, parallel or platform, to describe scar patterning and the particular techniques used to exploit the volume of cores.

Even such dedicated and elaborate descriptions of scar patterning will encounter problems dealing with cores that are complex or have scar patterns that fall outside, or in between, these categories. As with other core typologies, the description of scar patterning used in these systems also cannot be easily disentangled from core shape. A great deal of subjectivity and ambiguity is therefore encapsulated within idealized typological descriptions of cores. The definitions and exhaustiveness of a typology will help determine to what degree such ambiguity exists, but a quantitative measure such as the one proposed here need not make such complex and subjective classificatory decisions. All scars, whether typical or atypical of certain forms, will be automatically factored into the final result. In this way, the technique explored in this paper is a significant improvement on traditional descriptive methods.

Furthermore, while human pattern-recognition skills can sometimes be accurate as well as very fast, it is nevertheless difficult to extend qualitative observations of patterning for a single object to the detailed and reliable comparison of many, particularly when several researchers are involved, the objects are not all available at the same time and observations are separated by long time intervals. Quantitative description helps overcome these difficulties by making all comparisons on the same

terms, irrespective of who is undertaking the analysis or the size of the time gap between observations. Although our analysis is limited to a study of scar patterning and does not take into account such variables as core shape, platform preparation etc., future applications may easily combine scar pattern measures with other measures to provide a robust and holistic quantitative description of core technology.

In the remainder of this paper we develop procedures for quantifying scar patterns that should be applicable in any lithic analysis provided one has access to a Microscribe-3DX digitiser (or similar digitising instrument). The following sections work toward developing a single effective measure of scar patterning that could be applied in any analysis of core form and reduction technology.

### 3. Three-dimensional recording of flake scars on cores

Deriving a robust measure of flake scar patterning first requires the recording of negative flake scars in three dimensions so that their size and orientation in relation to one another can be calculated. The procedure adopted for obtaining these data was to use a three-dimensional digitiser – a stylus attached to a manoeuvrable mechanical arm that obtains three-dimensional coordinates for any desired point within reach (Fig. 2) – to record in three dimensions the start and end points for all intact and truncated scars found on the surfaces of cores (Fig. 3). The location of the stylus tip is



Fig. 2. A Microscribe-3DX, or digital recording device used to measure points in three-dimensional space. The arrow points to the tip of the stylus used to record start and end points for each scar.

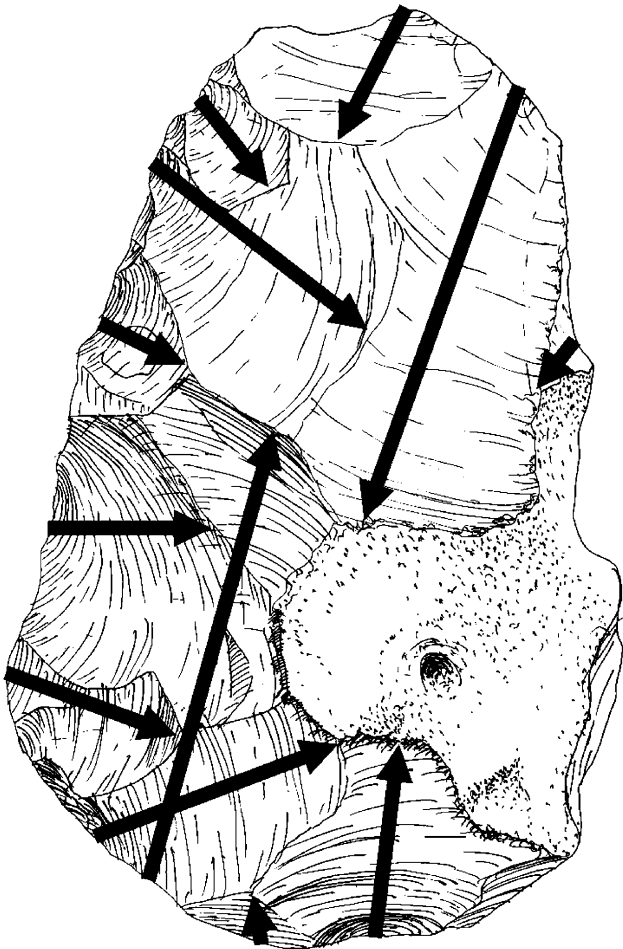


Fig. 3. Start and end points are recorded for each complete and truncated flake scar greater than 1 cm in length.

recorded in three dimensions every time the capture button is pressed. The *Inscribe32* software, which is freely available on the Internet, provides the interface between the digitiser and the computer's data handling software, and allows these data to be automatically entered into a spreadsheet or database. We chose to use *Microsoft Excel* in this case.

During this first step of digitising scar locations, the artefact must be immobilised so that the coordinates for the start and end points of each flake scar can be correctly tied into the Microscribe's datum, ensuring that scars are recorded in their proper position relative to one another. In our experiments, this was best achieved through the use of a large ring of blue tack stuck to a bench top, into which an artefact was pressed. Because the artefact cannot be moved during recording, it is usually necessary to measure cores in two halves. Software packages exist that are capable of joining the two halves back together again at the end of the recording phase (e.g. *Morpheus* and *Morphologika* packages) provided consistent 3D landmarks are recorded, however, this was not undertaken in this

analysis. All subsequent calculations leading to a measure of scar patterning presented later in this paper are therefore derived from the mean of the two halves measured separately.

Dividing a core into two symmetrical halves is not difficult when a clear plane of intersection between two domed surfaces exists, such as for bifacially flaked biconical cores like handaxes, discoids and Levallois cores. It is more difficult to define clear halves for irregular cores, or those that are more or less spherical, conical or cylindrical in shape. Because such cores often do not possess a clear line of intersection between two symmetrical halves, and because they lack universal landmarks or surfaces that allow specimens to be oriented in the same way each time, it is necessary to follow a set of guidelines to help ensure accurate and repeatable results are obtained. Several approaches are possible, but two rules were followed in this experiment. These were that partitioning into halves should aim to capture a similar number of flake scars in each half (except where a distinct cortical or non-flaked surface equal to roughly half the surface area of the core exists), and that partitioning should cross-cut the percussion axis of scars as little as possible. For example, a conical blade core would be divided into a front and back half so as not to cross-cut the alignment of the parallel flaking typical of a blade core, and the partition would therefore run through the long axis of the cone from the point to the centre of the flat base (platform), rather than truncating the cone halfway along its long axis, which would result in cutting the elongate flake scars in half. Results will vary somewhat depending on where exactly the partition is placed, and which scars are included, but the differences between observers should be minimal.

When a core displayed centripetal flaking on one surface and parallel flaking on the other, we were also careful to keep the two halves separate so as not to cross-cut or truncate the parallel flake scars and alter the scar pattern result for the parallel flaked surface unnecessarily. Cores that have one surface flaked and another that is cortical or left unflaked can be recorded as a single surface and the result for this surface used as the mean for both sides.

#### 4. Calculating a scar pattern index using vector analysis

The next step was to derive an index of overall scar pattern on the cores. The most appropriate analytical method for calculating this index is vector algebra. A three-dimensional vector is a numerical representation of spatial movement (Fig. 4). In a Cartesian system, its three coordinates (one for each dimension) define an arrow connecting a start and an end position, thereby conveying information on both magnitude and direction

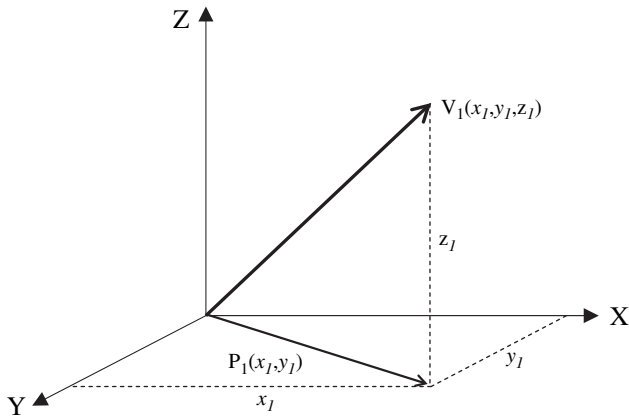


Fig. 4. Vectors represent positional change. The three-dimensional vector  $V_1$  is defined by the coordinates  $(x_1, y_1, z_1)$ . The size of  $P_1$  (the projection of  $V_1$  on two dimensions) is  $|P_1| = \sqrt{x_1^2 + y_1^2}$ . Therefore, the size of  $V_1$  is given by  $|V_1| = \sqrt{|P_1|^2 + z_1^2} = \sqrt{x_1^2 + y_1^2 + z_1^2}$ .

of spatial displacement. For this reason, vectors were used to represent start, end, size and direction of scars on a core.

Using the appropriate interface software, the Microscribe automatically enters  $x, y, z$  points for the start and end points of each scar (Table 1). To obtain a vectorial representation of each scar, the end point coordinates are then subtracted from the start point coordinates as shown in Table 1. The three resulting coordinates define a vector representing the magnitude and direction of the scar (Fig. 4).

An appropriate index of scar patterning can be obtained from only two quantities derived from the set of vectors representing scars on a core. The two measures can be easily understood by the use of an example. Suppose a subject takes a walk consisting of a number of steps in a given direction interspersed with rotations (for example, three steps to the south, then a  $30^\circ$  rotation to the left, then five steps, then another rotation), until they amount to 100 steps. The ‘distance walked’ is in this case 100 steps. The ‘displacement from the origin’, on the other hand, is a vector whose magnitude and direction depends on the walk taken by the subject. The ‘distance from the origin’, or magnitude

of that vector, will range from around zero (if the walk is truly random) to one (if the walk is a straight line from the origin). As seen below, our method excludes situations where a ‘zero sum’ could be produced by non-random walks (for example, if the subject walks 50 steps in one direction, rotates  $180^\circ$ , and then returns to the origin).

Importantly, ‘distance walked’ and ‘distance from origin’ can be readily associated with the main properties of scar distribution. ‘Distance walked’ stands for the summed length of all the scars on a core. ‘Displacement from origin’ is the resulting ‘walk’ of all scars on the surface of the core, or a vector that describes the overall directional tendency of the scars, and ‘distance from origin’ is the magnitude of this vector. Both resulting vector size and total scar length can be easily calculated. The resulting vector summarising scar directional tendency on a core is the sum of all the  $x, y$  and  $z$  coordinates for all the scars, and its magnitude (or norm) is obtained by the Pythagoras theorem as the square root of the summed squared coordinates. Total scar length is the sum of the norms of all individual scar vectors (Fig. 5). As seen in the following, the ratio of resultant vector size (‘distance from origin’) to total scar length (‘distance walked’) exhibits the appropriate properties of a scar patterning index.

The ratio quantifies, on a scale of zero to one, scar orientation in the continuum from random (zero) to totally patterned (one). We interpret scar patterning as a measure of the degree to which scars are aligned in a single direction; the ratio or index is therefore a measure of parallelness. One sees that, when the resulting vector is zero, scar patterns must all have cancelled each other out, such as when they are randomly aligned over the surface of a core (Fig. 6, top), and the index value will be close to zero. If resulting vector size is the same as total scar length, then it must be the case that all scars are aligned in exactly the same direction, and the index value will be one. In intermediate cases, where the resulting vector falls short of the sum of scars, the patterning of scars can be seen to be intermediate between a totally random scar pattern and a parallel one. An example of an intermediate scar

Table 1  
Procedure for deriving vectors from scar start and end points

Start			End			
$x_1$	$y_1$	$z_1$	$x_2$	$y_2$	$z_2$	
205.7	-77.7	58.4	193.3	-94.8	64.8	Coordinates obtained from the microscribe
			12.4	17.1	-6.5	Start point – end point
			154.4	292.6	41.6	Residual squared
			488.6			Sum of squared residuals
			22.1			Square root of sum of squared residuals

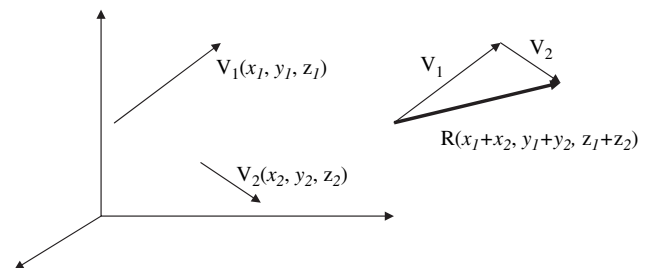


Fig. 5. Sum of vectors. Given two vectors  $V_1(x_1, y_1, z_1)$  and  $V_2(x_2, y_2, z_2)$ , the resultant vector  $R(x_1 + x_2, y_1 + y_2, z_1 + z_2)$  is the sum of  $V_1$  and  $V_2$ , and represents their net effect in terms of positional change.

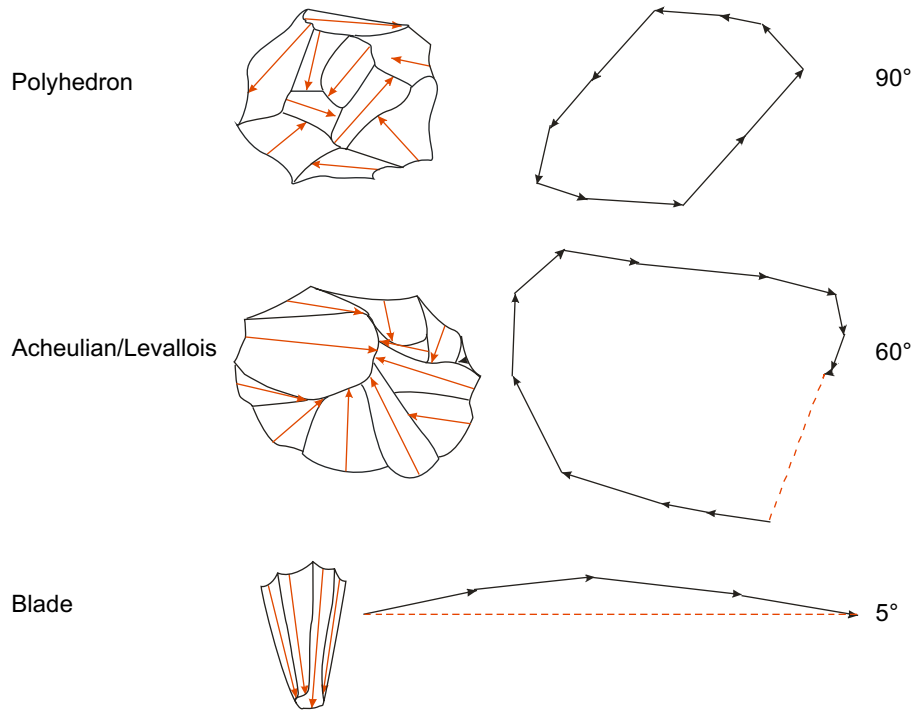


Fig. 6. Illustration of the degree to which flake scar trajectories can cancel each other out and decrease the resultant displacement. The illustration in the middle represents the ‘distance walked’ and the dashed line the ‘distance from origin’, or the overall magnitude and directional tendency of all vectors. This is expressed as an angle as shown at the right of the diagram.

pattern would be a slightly domed, centripetally flaked core, in which scars shared a common trajectory toward the apex of the dome, but also cancelled each other out to some degree by meeting in the middle. It should be noticed that the method of registering scars from only each half of a core separately guarantees that a resulting vector with size close to zero necessarily results from random scar orientation, instead of a symmetrical scar arrangement (for example, if scars from each half of the core cancel each other out).

### 5. Converting vectors into an angle of scar pattern alignment

The patterning index can be converted into an angle representing the overall distribution of scars on a core. If we interpret the size of the resulting vector (‘distance from origin’) as a projection or fraction of total scar length (‘distance walked’), the index becomes a cosine corresponding to an angle of projection (Fig. 7). In other words, if a subject walks 100 steps but ends up only 50 steps from the origin, this can be interpreted as the result of the subject having walked not straight but ‘at an angle’ to a target position 100 steps away, consequently wasting 50 steps. In this case, the patterning index is 0.5, a cosine corresponding to an angle of 60° (for our purposes, 10°, 350° and –10° represent the same relative orientation

between two scars, and are represented as 10°. Therefore, all angles are defined in the interval 0–180°).

Importantly, it can be shown that the projection angle is also the average or expected angle obtained if one selects two scars randomly from a core (Fig. 7). An index or cosine of one corresponds to a 0° angle, i.e. to

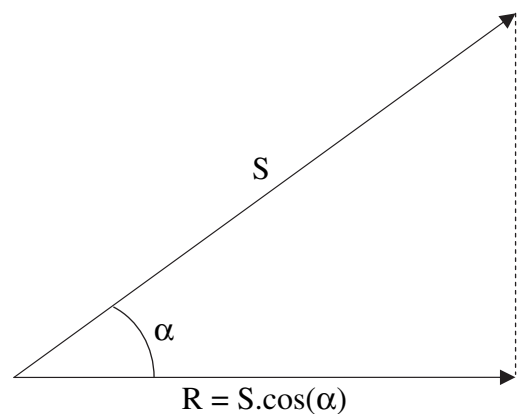


Fig. 7. The index of parallelness. The total length of a set of vectors (or ‘distance walked’) is the sum of all vector sizes, or  $|S| = \sum |V_i|$ . The resultant vector  $R$  is the sum of the coordinates of all vectors, or  $R = (\sum x_i, \sum y_i, \sum z_i)$ . The size of the resultant vector, or ‘distance from origin’, is therefore  $|R| = \sqrt{[(\sum x_i)^2 + (\sum y_i)^2 + (\sum z_i)^2]}$ . If one interprets the index  $|R|/|S|$  as a cosine,  $R$  becomes a projection of  $S$ , and  $\alpha$  becomes a measure of the average angle between any two vectors in the set.

parallel scars. Since negative angles are excluded, an average of zero implies that all angles between any two scars are also zero. Therefore, if the index is one ( $0^\circ$ ), any two scars picked at random will be oriented in the same direction (i.e. parallel): given a first scar, the direction of the second one is predictable with total certainty. On the other hand, if the index is zero, the corresponding angle is  $90^\circ$ . This angle is the average from a random distribution of angles ranging from  $0^\circ$  (parallel scars) to  $180^\circ$  (diametrically opposed scars). In intermediate cases such as the one described in the previous paragraph, an index of 0.5 means that the expected or average angle between any two scars is  $60^\circ$ .

Finally, the angle derived from the patterning index is weighted by the size of each scar, such that the effects of a few small scars at random orientation will be overridden by a few large scars oriented in a single direction. This is potentially advantageous in that it may downplay the effects of many small scars that derive from, say, preparation of the core platform, rather than longer scars that give the core its overall shape.

## 6. The experimental case study

To test how well this procedure works on cores with differing scar patterns, the scars on 55 cores were recorded using the Microscribe-3DX, converted into vectors and a scar pattern angle calculated for each half of each core. Both experimental and archaeological cores were used in this analysis, and cores were selected that fit into four main categories, roughly following Clark's [7] technological 'modes' (Table 2). Polyhedrons are roughly spherical cores flaked on many sides in a non-systematic, heavily rotated fashion. These coincide with Clark's Mode 1 technology. Acheulian handaxes are flaked in a radial pattern around the circumference of both faces and fit Clark's Mode 2. Levallois/disoidal cores are also flaked in a radial fashion, but are more clearly centripetal in flake scar orientation than handaxes, which tend to be pointed or ovate and possess a more attenuated scar pattern. These cores fit within Clark's Mode 3 technologies. Finally, a number of conical and cylindrical blade cores were selected to represent scar patterns that are predominantly aligned in a single direction and are often close to parallel. These cores fit Clark's Mode 4 technologies.

Not only are Clark's modes useful in enabling the characterisation of scar patterns that mirror, in general, terms, the evolution of stone-working technologies since their inception more than 2 million years ago, but they have also been recently embraced as a convenient heuristic with which to investigate patterns of hominin dispersal and long-term technological continuity and change [18,19,23]. In reality though, developing methods for quantifying core morphology allows us to move

beyond such broad categories as modes to more detailed inter-assemblage comparisons at varying scales. Therefore, one of the main aims of the study is to define a quantitative approach to archaeological cores that would allow analysing spatial and temporal patterns independent of such a simplistic categorical system.

Because the methods for calculating scar pattern angle calculate an average from the direction and magnitude of several scars, we have chosen to use cores with many scars on their surfaces. In principle, this technique could be used to record a single flake scar, but of course these cores would all have a scar pattern angle of  $0^\circ$ , and may be of little value in characterising the nature of reduction technology when compared to more heavily flaked specimens. We would therefore recommend including only cores with at least three scars in such analyses. We also acknowledge that the measured sample of cores was selected to emphasise the differences between core types and that other kinds of cores may show results that are more intermediate between those we obtained.

## 7. Results

To present the results of the experiment, a box plot is shown in Fig. 8 that describes the distribution and central tendency of the mean scar pattern angles of cores for each group. It can be seen from Fig. 8 that there is a consistent progression from blade cores at the bottom left, to polyhedrons at the top right of the graph. This trend fits the expectations of the model given that blade cores are expected to have low scar pattern angles since scars should tend towards parallel alignment oriented in a single direction, while polyhedrons with near-random patterns of flake scar alignment should have high scar pattern angles. It should be pointed out that angles of  $90^\circ$  or  $0^\circ$  will likely be very rare since few scar patterns will be truly random (i.e. where all vectors are completely cancelled out) or truly parallel (i.e. where all scars are aligned in exactly the same direction). We should therefore expect the actual range of scar pattern angles to be more like that seen in Fig. 8.

Interestingly, cores with radial flake scar patterns also meet theoretical expectations by fitting neatly between blade cores and polyhedrons as opposite ends of the spectrum, with Disoidal/Levallois and Acheulian handaxes possessing scar pattern angles of between  $40^\circ$  and  $70^\circ$  (Fig. 8). While there are differences in the range of values for each of these radially flaked core forms — with Acheulian handaxes skewed more toward the random scar patterning end of the spectrum (probably due to their attenuated plan form resulting in more scars canceling each other out) and disoidal/Levallois cores showing a near normal distribution — their median values are almost identical. This observation seems to lend weight to

Table 2  
Details of the 54 cores used in the scar pattern experiment

Specimen	Raw material	Typology	% Blade scars	Angle top	Angle bottom	Mean scar pattern angle	Scar pattern angle squared
1	Flint	Acheulian handaxe	2.8	55	69	62	3838
2	Flint	Acheulian handaxe	10.8	51	53	52	2708
3	Flint	Acheulian handaxe	6.9	51	63	57	3267
4	Obsidian	Acheulian handaxe	4.8	60	64	62	3846
5	Obsidian	Acheulian handaxe	1.9	55	60	58	3313
6	Flint	Blade core	35.7	28	15	22	469
7	Flint	Blade core	83.3	5	57	31	948
8	Flint	Crested blade core	53.3	9	30	19	364
9	Flint	Blade core	100.0	14	19	16	271
10	Flint	Blade core	72.7	21	15	18	334
11	Flint	Blade core	71.4	21	23	22	480
12	Flint	Crested blade core	50.0	19	56	38	1418
13	Flint	Blade core	92.3	18	14	16	244
14	Flint	Blade core	77.8	15	4	10	92
15	Flint	Crested blade core	69.2	16	64	40	1610
16	Flint	Discooidal/Levallois core	13.8	56	52	54	2924
17	Flint	Discooidal/Levallois core	26.1	62	44	53	2783
18	Flint	Discooidal/Levallois core	12.0	58	65	62	3828
19	Flint	Discooidal/Levallois core	0.0	52	53	52	2744
20	Flint	Discooidal/Levallois core	0.0	63	41	52	2707
21	Flint	Discooidal/Levallois core	4.2	61	34	48	2291
22	Flint	Discooidal/Levallois core	6.3	52	61	56	3150
23	Flint	Polyhedron	8.3	75	84	80	6361
24	Flint	Polyhedron	6.7	80	67	73	5335
25	Flint	Polyhedron	3.7	72	78	75	5682
26	Flint	Polyhedron	0.0	81	53	67	4465
27	Flint	Polyhedron	0.0	66	75	70	4943
28	Flint	Blade core	51.9	5	54	29	860
29	Cast	Discooidal/Levallois core	18.9	62	39	50	2510
30	Flint	Acheulian handaxe	2.8	40	63	52	2667
31	Flint	Acheulian handaxe	2.8	42	58	50	2476
32	Flint	Acheulian handaxe	2.7	54	44	49	2418
33	Flint	Acheulian handaxe	2.2	51	46	48	2324
34	Flint	Acheulian handaxe	6.5	63	56	60	3571
35	Flint	Acheulian handaxe	0.0	74	66	70	4872
36	Flint	Acheulian handaxe	0.0	40	59	50	2464
37	Flint	Polyhedron	0.0	79	59	69	4738
38	Flint	Polyhedron	0.0	62	72	67	4519
39	Flint	Crested pressure blade core	38.9	7	44	26	653
40	Flint	Pressure blade core	100.0	3		3	9
41	Flint	Polyhedron	0.0	77	79	78	6076
42	Flint	Polyhedron	0.0	81	60	70	4939
43	Flint	Polyhedron	6.7	61	54	58	3325
44	Flint	Discooidal/Levallois core	3.8	61	47	54	2932
45	Flint	Discooidal/Levallois core	5.6	50	35	43	1814
46	Flint	Discooidal/Levallois core	0.0	66	43	54	2960
47	Flint	Discooidal/Levallois core	3.6	62	40	51	2612
48	Flint	Discooidal/Levallois core	4.3	64	47	56	3104
49	Flint	Acheulian handaxe	0.0	57	51	54	2943
50	Flint	Discooidal/Levallois core	7.7	53	39	46	2148
51	Flint	Discooidal/Levallois core	4.0	62	39	51	2565
52	Flint	Discooidal/Levallois core	14.3	62	40	51	2632
53	Flint	Discooidal/Levallois core	6.9	58	50	54	2916
54	Flint	Discooidal/Levallois core	0.0	51	38	45	1994

the argument for a strong similarity in the flaking techniques employed in these two technologies [35].

Scar pattern angle alone, however, is unable to provide an entirely satisfactory level of separation between core types, since they tend to bunch up toward

the middle and top of the scale. This effect can be easily overcome by squaring the scar pattern angle. The mean and standard deviations obtained for each set of cores once this transformation has been performed are shown in Fig. 9. At one standard deviation, the degree of

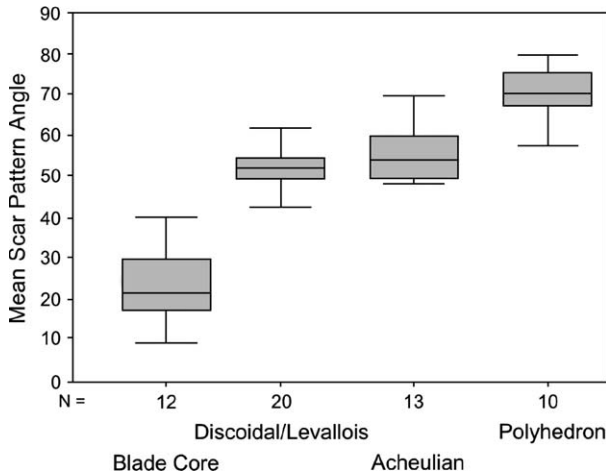


Fig. 8. Results of the conversion of vectors into an angle expressing scar patterning for common core types.

separation between cores with different scar patterns is total, demonstrating that scar pattern angle is an effective means of measuring and distinguishing between such clearly different scar patterns. A one way ANOVA confirms that the overall difference in means is statistically significant ( $F = 137.07$ ,  $df = 3$ ,  $p < 0.005$ ), although the difference in means between Discoidal/Levallois cores and Acheulian handaxes is not significant ( $p = 0.907$ ).

Another test of the utility of this index is to plot the percentage of elongate (length:width > 2:1) parallel scars (i.e. ‘blade scars’) against the scar pattern angle for the population of cores used in the experiment (Fig. 10). The result indicates that cores with high numbers of elongate parallel scars are readily separated using this index, and that scar pattern angle is effective

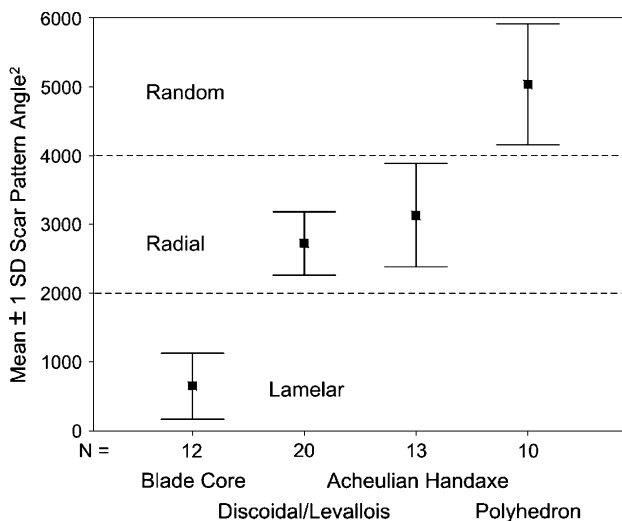


Fig. 9. Results obtained when mean scar pattern angle is squared.

in picking up differences in scar size, shape and alignment at this scale of analysis.

As mentioned previously, this study makes use of vectors for both the complete and truncated scars found on cores. It is worth finally considering what effect the use of less ambiguous flake scars, such as those that retain a clear point of initiation and termination, would have on the scar pattern results. Examining complete scars means recording fewer scars, but in so doing increases the level of certainty about start and end points for all measured scars. A comparison of the scar pattern angles resulting from using complete and truncated scars versus complete scars only reveals that the two techniques, though yielding significantly different results ( $t = -2.76$ ,  $p = 0.011$ ), closely match one another. A regression analysis, for instance, indicates that the results for both techniques strongly co-vary ( $r^2 = 0.945$ ,  $p < 0.0005$ ), with as little as 4.5% of variation arising from the use of different techniques. While these closely matching results indicate that it may be worth the added rigour of recording only complete scars in many cases, in fact many cores have so few scars that eliminating truncated ones could critically alter scar pattern results, and complete scars may not always accurately mirror the overall scar pattern. This would commonly be the case, for example, for heavily rotated polyhedrons where scars sequentially added from new platforms around the surface of the core would truncate many or most of the already existing scars. We therefore recommend recording truncated as well as complete scars to gain a better overall depiction of flake scar patterning.

### 8. Conclusion

Our 3D analysis of scar patterning on core surfaces has yielded very encouraging results, and suggests that

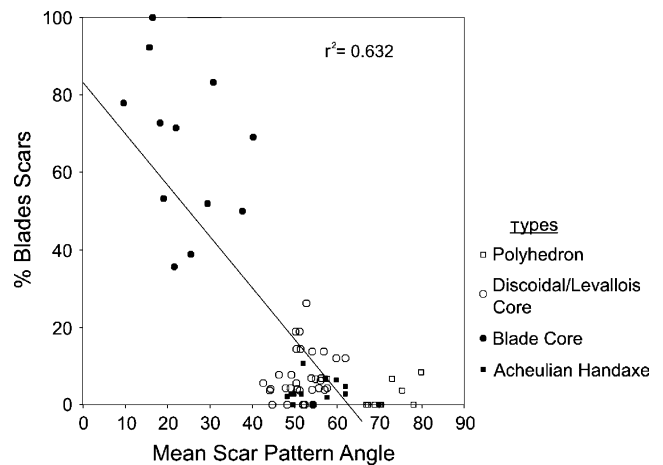


Fig. 10. Regression analysis of the percentage of blade scars (elongate, parallel sided scars with length:width > 2:1) found on each core plotted against the scar pattern angle for each core.

this measure could be adopted in many lithic analyses to better characterize variability in core reduction strategies. It would appear that this technique can be successfully applied to most cores, and that it is not overly sensitive to variation in recording techniques. If the same guidelines used in this experiment are applied in all applications of the method, it should also be quite resilient in terms of inter-observer error. Three-dimensional digitisers are still expensive items, but judging from the ever-falling price of computers, they should be very affordable soon. Their ability to capture many features of complex three-dimensional objects also suggests they should prove very useful in developing other quantitative measures of artefact morphology and technology that are beyond the capability of traditional measurement techniques. We believe 3D recording of stone artefacts offers the most promising method currently available for capturing the complexity and diversity of chipped stone artefacts, and hope such techniques will see intensive development in coming years.

An extension to the procedures presented in this paper which was not developed here, would be the use of this method in quantifying scar patterning on the dorsal surfaces of flakes. Although there may be limitations when applied to flakes – such as a fewer scars, flatter profiles and less complexity overall – this technique should be applicable in measuring dorsal scar patterns, and may be an extremely useful means of describing modes and variation in flake production between assemblages.

Stone artefacts hold great promise for investigating issues pertaining to human origins, past landuse practices, adaptation and cultural change. Appropriate methods for quantifying morphology and technology are emerging at a steadily increasing pace, as is the explication of the theoretical principles that provide connections between the patterned material record, past behaviour, cognitive development, human sociality and the nature of causation. A truly comprehensive and satisfying corpus of techniques for investigating the many significant issues surrounding the evolution of lithic technology may still be some years in coming; however, there are encouraging signs that this is achievable. We hope three-dimensional morphometric techniques are adopted by other researchers and continue to be developed in the years to come.

### Acknowledgements

This research was carried out as part of the project “Searching for traces of the Southern Dispersal”, funded by the UK National Environmental Research Council (NERC-EFCHED Programme). We would

also like to thank R.A. Foley for comments and suggestions.

### References

- [1] D.C. Adams, F.J. Rohlf, D.E. Slice, *Ital. J. Zool.* 71 (2004) 5–16.
- [2] S.A. Ahler, in: D.O. Henry, G.H. Odell (Eds.), *Alternative Approaches to Lithic Analysis*, Archaeological Papers of the American Anthropological Association 1, 1989, pp. 85–118.
- [3] R.J. Austin, *Lith. Technol.* 24 (1997) 53–68.
- [4] L.S. Barham, *The Middle Stone Age of Zambia*, Western Academic and Specialist Press, Bristol, 2000.
- [5] M.F. Baulmer, in: H. Dibble, A. Montet-White (Eds.), *Upper Pleistocene Prehistory of the Western Eurasia*, University of Pennsylvania, Philadelphia, 1988, pp. 255–274.
- [6] J.D. Clark (Ed.), *Kalambo Falls Prehistoric Site*, vol. 3, Cambridge University Press, Cambridge, 2001.
- [7] J.G.D. Clark, *World Prehistory: A New Outline*, Cambridge University Press, Cambridge, 1968.
- [8] C. Clarkson, *J. Archaeol. Sci.* 1 (2002) 65–75.
- [9] N.J. Conard, M. Soressi, J.E. Parkington, S. Wurz, R. Yates, *S. Afr. Arch. Bull.* 59 (2004) 13–17.
- [10] B. Cotterell, J. Kamminga, in: B. Hayden (Ed.), *Lithic Use-wear Analysis*, Academic Press, New York, 1977.
- [11] B. Cotterell, J. Kamminga, *Am. Antiq.* 52 (1987) 675–708.
- [12] B. Cotterell, J. Kamminga, *Mechanics of Pre-industrial Technology*, Cambridge University Press, Cambridge, 1990.
- [13] A. Debénath, H.L. Dibble, *Handbook of Paleolithic Typology*, University Museum, University of Pennsylvania, Philadelphia, 1994.
- [14] H. Dibble, P. Chase, *Am. Antiq.* 46 (1981) 178–187.
- [15] H. Dibble, A. Pelcin, *J. Archaeol. Sci.* 22 (1995) 429–439.
- [16] H. Dibble, J. Whittaker, *J. Archaeol. Sci.* 6 (1981).
- [17] A. Faulkner, PhD thesis, Washington State University, University Microfilms, Ann. Arbor. (1972).
- [18] R. Foley, M. Mirazon Lahr, *Evol. Anthropol.* 12 (2003) 108–122.
- [19] R. Foley, M.M. Lahr, *Camb. J. Archaeol.* 7 (1997) 3–36.
- [20] J. Gunn, in: J.N. Hill, J. Gunn (Eds.), *The Individual in Prehistory: Studies of Variability in Style in Prehistoric Technologies*, 1977, pp. 167–204.
- [21] S. Kuhn, *J. Archaeol. Sci.* 17 (1990) 585–593.
- [22] S. Kuhn, *Am. Antiq.* 57 (1992) 115–128.
- [23] M.M. Lahr, R.A. Foley, in: L. Barham, K. Robson Brown (Eds.), *Human Roots: Africa and Asia in the Middle Pleistocene*, Western Academic & Specialist Press, Bristol, 2001, pp. 23–39.
- [24] O. Macgregor, in: C. Clarkson, L. Lamb (Eds.), *Lithics Down Under: Australian Perspectives on Lithic Reduction, Use and Classification*, Archaeopress, Oxford, in press.
- [25] S. McPherron, H. Dibble, *Lith. Technol.* 24 (1999) 38–52.
- [26] T.A. Morrow, *Lith. Technol.* 22 (1997) 51–69.
- [27] G.H. Odell, in: D.S. Amick, R.P. Mauldin (Eds.), *Experiments in Lithic Technology*, British Archaeological Reports, Oxford, 1989, pp. 163–198.
- [28] L.W. Patterson, *Lith. Technol.* 11 (1982) 50–58.
- [29] L.W. Patterson, *Am. Antiq.* 55 (1990) 550–558.
- [30] L.W. Patterson, J.B. Sollberger, *Plains Anthropol.* 23 (1978) 103–112.
- [31] A. Pelcin, *J. Archaeol. Sci.* 24 (1997) 749–756.
- [32] A. Pelcin, *J. Archaeol. Sci.* 24 (1997) 1107–1113.
- [33] A. Pelcin, *J. Archaeol. Sci.* 25 (1998) 615–620.
- [34] F.J. Rohlf, L.F. Marcus, *Trends Ecol. Evol.* 8 (1993) 129–132.
- [35] N. Rolland, in: H.L. Dibble, O. Bar-Yosef (Eds.), *The Definition and Interpretation of Levallois Technology*, Prehistory Press, Madison, 1995, pp. 333–359.

- [36] I. Saragusti, A. Karasik, I. Sharon, U. Smilansky, *J. Archaeol. Sci.* 32 (2005) 841–853.
- [37] M.J. Shott, *Lith. Technol.* 21 (1996) 6–22.
- [38] J.D. Speth, *Am. Antiq.* 37 (1972) 34–60.
- [39] J.D. Speth, *Am. Antiq.* 40 (1975).
- [40] J.D. Speth, *Lith. Technol.* 10 (1981) 16–21.
- [41] J.D. Speth, *Tebiwa* 17 (1974) 7–36.
- [42] D.W. Stahle, J.E. Dunn, *World Archaeol.* 14 (1984) 84–97.
- [43] A. Steffen, E.J. Skinner, P.W. Ainsworth, in: A. Ramenofsky, A. Steffen (Eds.), *Unit Issues in Archaeology*, University of Utah Press, Salt Lake City, 1998, pp. 131–146.